

Mode Locking of a Novel Split-Contact Semiconductor Laser— Experiment and Theory

Craig A. Williamson and Michael J. Adams

Abstract—A novel semiconductor laser, with a curved and tapered active region and a split contact, has been experimentally and theoretically mode-locked for the first time. An innovative yet simple traveling-wave rate-equation model has been developed to incorporate the tapered waveguide structure together with external-cavity grating effects and the reverse biased saturable absorber region. Both the experiment and model have demonstrated pulsewidths of around 5.5 ps at a repetition frequency of 2.5 GHz and a tunable emission wavelength around 1550 nm. The model has been used to demonstrate optimized operation of the device with a predicted reduction in pulsewidths down to 1 ps.

Index Terms—Laser absorbers, mode-locked lasers, optical pulse generation, semiconductor device modeling, semiconductor lasers.

I. INTRODUCTION

PICOSECOND optical pulses are required for many applications including micromachining, medical imaging, and optical communications. The technique of mode locking can be used to generate such pulses from lasers, with pulse emission occurring at the round-trip frequency of the laser cavity. For present-day telecommunications use, repetition frequencies of the order of gigahertz are required, and in the context of semiconductor lasers this can be achieved through external cavity configurations.

In such a system, it is desirable to have high reflectivity at the semiconductor laser's output facet while having a very low reflectivity at the inner facet to couple to the external cavity. Inner facet reflectivities of the order of 10^{-6} are needed to suppress the formation of unwanted subpulses that can be generated due to internal reflections of the primary pulse [1].

The authors have previously reported [2] the active mode locking of a semiconductor laser with a curved waveguide to reduce the reflectivity at only one facet and an active region that tapers down toward this facet in order to allow the guided mode to expand into an underlying passive waveguide and further reduce the reflectivity to 8×10^{-6} [3]. The expanded mode also improves coupling efficiencies and relaxes alignment tolerances out into the external cavity [4], and the device is, therefore, ideal for external cavity operation.

Manuscript received September 17, 2003; revised March 24, 2004. This work was supported by EPSRC and Corning.

The authors are with the Department of Electronic Systems Engineering, University of Essex, Colchester CO4 3SQ, U.K. (e-mail: craig@williamson.name; adam@essex.ac.uk).

Digital Object Identifier 10.1109/JQE.2004.830180

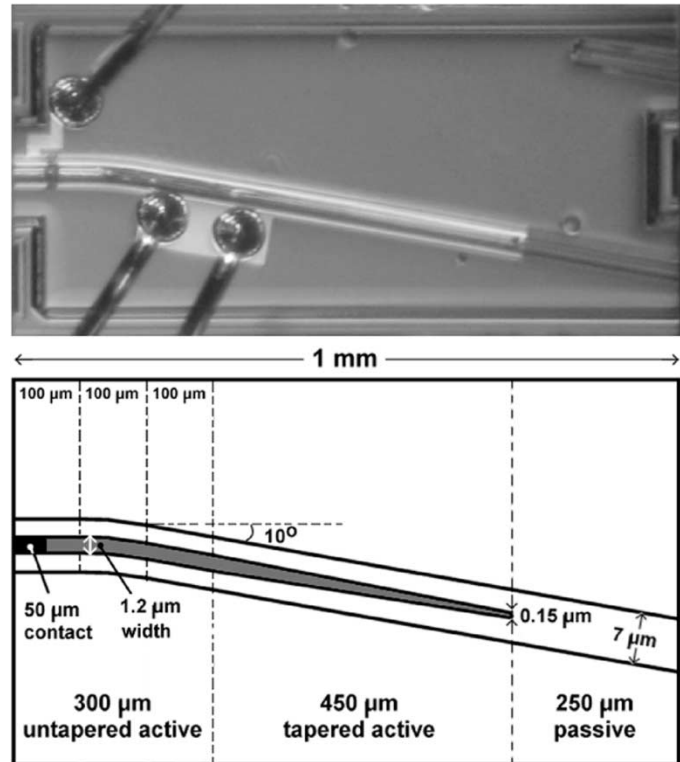


Fig. 1. Top-view photograph (top) and schematic diagram (bottom) of the split-contact device.

This study focuses on the hybrid mode locking of a split contact variation of the device, which retains the unique features that are essential for external cavity operation while having the potential for reduced pulsewidths due to the effects of saturable absorption. To support the experimental work, an innovative model has been developed that allows the complicated effects of the tapered structure, external cavity grating, and reverse-biased saturable absorber region to be simulated by a simple approach. To our knowledge, this is the first time such a laser design has been reported in the mode-locking regime.

II. DEVICE DESIGN

The device is based upon a 1550-nm InGaAsP multiple-quantum-well (MQW) buried-heterostructure device first reported in 1998 for use as a fiber grating laser (FGL) [3]. Fig. 1 shows the top-view of the laser structure, which begins with a 100- μm straight untapered active section of 1.2 μm

in width, with the first 50 μm having a separate electrical contact to the remainder of the active region. The waveguide curves over the next 100 μm to a final angle of 10° , and then continues for the next 100 μm with a 1.2- μm width giving a total untapered active region of approximately 300 μm in length. Next, a 450- μm active section tapers down to a width of 0.15 μm , and the guided mode expands into the underlying passive waveguide of 7- μm width. The final section of 250 μm is purely passive and gives a total chip length of 1 mm, with the angled facet and increased waveguide width serving to reduce the facet reflectivity to 8×10^{-6} .

The active region comprises eight quantum wells (QWs) of $\text{In}_{0.84}\text{Ga}_{0.16}\text{As}_{0.68}\text{P}_{0.32}$ at 70- \AA thickness, compressively strained -1% with respect to the InP substrate. The seven barriers are 140- \AA -thick 1.3- μm InGaAsP with a tensile strain of $+0.5\%$, and at the top and bottom of the active region is a 100- \AA -thick separate-confinement heterostructure (SCH) of the same composition and strain as the barriers.

III. EXPERIMENT

A. External Cavity Configuration

A 2.5-GHz laser cavity is formed between the conventional facet of the semiconductor laser and a moveable grating, with a ball lens being used at the low-reflectivity facet to collimate the light into the external cavity. A tapered fiber is located at the conventional cleaved facet to take the light output to test equipment.

The grating only reflects a small (~ 1 nm) range of wavelengths from the 200 nm or so output spectrum of the device and allows tuning over a wavelength range of approximately 30 nm. Its distance from the laser, approximately 5.6 cm, can be adjusted in order to finetune the matching of the cavity round-trip frequency to the driving RF frequency.

B. Driving Conditions

The dc and RF are applied to the main contact of the active region, with 2.5-GHz operation being the focus of this work. The maximum available RF power at 2.5 GHz was 35 dBm, which was found to give the shortest pulses for any given dc bias level and was, therefore, used throughout the experiments. The 50- μm contact is connected to a voltage source, with the act of grounding the contact found to give saturable absorption effects that are required for hybrid mode-locking. This was identified by a sudden turn-on of output under increasing dc bias, together with bistable behavior. Erratic performance was experienced under reverse bias operation, which was attributed to a low isolation resistance between the two contacts. For this reason, the device was only grounded during mode-locking experiments.

C. Results

With the 50- μm contact left as an open-circuit, there is no through path for any leakage current and the section acts as a purely passive region. Pulses slowly build up with increasing dc bias levels from as low as 15 mA. With a dc bias of 50 mA and the maximum RF power at 2.5 GHz, the device was actively

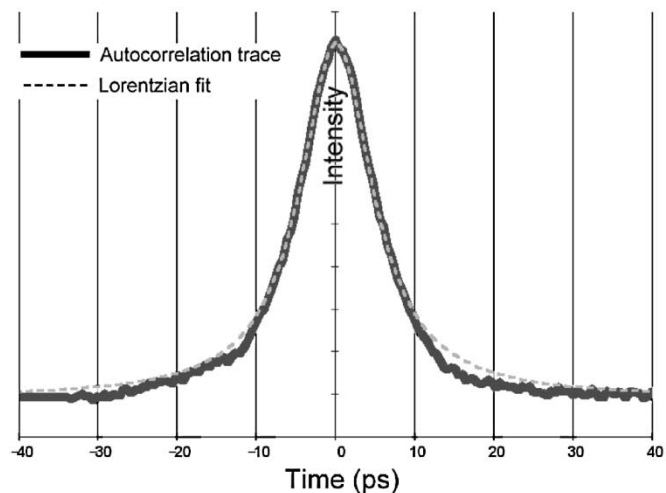


Fig. 2. Autocorrelation trace of the experimentally obtained pulse with a grounded 50- μm contact and dc bias of 70 mA, showing the best-fit autocorrelation function generated by a 5.6-ps Lorentzian actual pulse shape.

mode-locked and generated pulses with autocorrelation widths of 12.7 ps. The autocorrelation function best matches that generated by a Lorentzian actual pulseshape, although it should be noted that there is considerable uncertainty in such conversions [5]. Assuming Lorentzian pulses implies a pulsewidth of 6.4 ps, with the spectral linewidth being 1.03 nm and a time–bandwidth product of 0.83 (3.8 times the theoretical limit). Such results are comparable to those previously reported for the single-contact device [2], and the effects of having this 50- μm region as passive rather than active does not appear to make any distinguishable difference to the results.

When the second contact of the device is grounded, there is a noticeable change in the mode-locking behavior. The pulses switch on very suddenly at a dc bias of around 40 mA, giving autocorrelation widths of 12.1 ps, without the gradual build-up of pulses that was evident in the open circuit case. This indicates that there is an absorption function occurring within the laser and at the 40-mA dc bias level it is being saturated, thus allowing pulses to be emitted.

Fig. 2 shows the autocorrelation trace obtained with a grounded contact at a dc bias of 70 mA with a full-width at half-maximum power of 11.2 ps. A Lorentzian actual pulse shape is assumed, giving a pulse width of 5.6 ps. The spectral linewidth was 1.49 nm, resulting in a time–bandwidth product of 1.05 that is 4.8 times the limit for Lorentzian pulses.

Grounding the 50- μm contact clearly produced saturable absorption effects and so hybrid mode-locking was taking place. However, the improvement in pulse widths compared to the actively mode-locked single-contact case were not significant, and so a model has been developed to investigate whether reverse biasing the contact could be expected to improve the pulse performance to a greater extent.

IV. MODEL PRINCIPLES

The model uses a traveling-wave rate-equation approach, which involves the solution of rate equations in time and position to build up an accurate profile of the carrier and photon

densities throughout the cavity and their development over time. The methodology of moving through the laser cavity step-by-step particularly lends itself to the device being used in this work that has a spatial variation in its active waveguide and, therefore, a variation of its associated properties. This similarly applies to the insertion of saturable absorber regions. The inclusion of a tapered waveguide, together with the effects of an external cavity grating, have not previously been reported in relation to a traveling wave rate equation model of the mode-locking of semiconductor lasers. Neither has a straightforward application of a saturable absorber for hybrid mode-locking created via a two-contact structure. It is hoped that the approach described herein can be seen as a simple yet effective method for modeling such systems.

A. Traveling-Wave Rate Equations

The foundations for the model are provided by published work from Demokan [6] and Bowers *et al.* [7]. Both works simulate the active mode-locking of semiconductor lasers with bulk active regions of constant width and external cavities incorporating conventional mirrors. Therefore, considerable efforts have been made to adapt them for application to this device.

The basic rate equations for electron density n and photon density S with respect to time t and position along the cavity x are given by

$$\frac{\partial n(x,t)}{\partial t} = \frac{J(t)}{ed} - (An^3 + Bn^2 + Cn) - \frac{c}{\eta} g_m (S^+ + S^-) \quad (1)$$

$$\frac{\partial S^\pm(x,t)}{\partial x} = (\Gamma g_m - \alpha_t) S^\pm + \frac{M\Gamma k \eta B}{c} n^2 \quad (2)$$

where S^+ and S^- represent the forward- and backward-propagating photon densities, respectively, $J(t)$ is the time-varying current density, e is the electronic charge, d is the thickness of the active layer, A is the Auger recombination coefficient, B is the band-to-band recombination rate, C is the trap recombination rate, c is the speed of light, η is the group refractive index, g_m is the material gain, Γ is the optical confinement factor, α_t is the total loss of the active region, M is the number of locked modes (estimated to be half the roundtrip time divided by the pulsewidth), and k is the spontaneous emission factor. Dispersion in the semiconductor material can be ignored for pulsewidths greater than 100 fs [7]. The applied current density is given by

$$J(t) = 0.5(J_{dc} + J_{rf} \sin(\omega t)) \quad (3)$$

where J_{dc} is the dc bias current density, J_{rf} is the peak RF current density, ω is the angular frequency of the RF corresponding to 2.5 GHz, and the factor of 0.5 is used as an approximate injection efficiency. J is not allowed to fall below zero in order to replicate the diode behavior of semiconductor lasers. The material gain is approximated by [8], [9]

$$g_m = g_0 \ln \left(\frac{n}{n_{tr}} \right) \quad (4)$$

TABLE I
DEVICE PARAMETERS

Parameter	Symbol	Value	Units
Active layer thickness	d	56	nm
Auger recombination coefficient	A	1.5×10^{-28}	cm^6s^{-1}
Band-to-band recombination rate	B	1×10^{-10}	cm^3s^{-1}
Trap recombination rate	C	1×10^8	s^{-1}
Group refractive index	η	3.7	
Optical confinement factor	Γ	0.079 – 0.006	
Spontaneous emission factor	k	2.8×10^{-5}	
Gain curve parameter	g_0	2935	cm^{-1}
Transparency electron density	n_{tr}	1.21×10^{18}	cm^{-3}
Free-carrier absorption coefficient within the active region	α_{fc}	5×10^{-18}	cm^2
Loss due to scattering	α_s	5	cm^{-1}
Free-carrier loss in the cladding regions	α_0	10	cm^{-1}
Loss in passive region	α_p	2	cm^{-1}
External facet reflectivity	R_1	0.28	
Grating reflectivity	R_2	0.7	
Internal facet reflectivity	R_3	8×10^{-6}	
External cavity coupling coefficient	C_c	0.3	

where g_0 is the gain curve parameter and n_{tr} is defined as the transparency electron density. Parameters for this approximation have been obtained experimentally as will be discussed in Section IV-C. The total loss is given by

$$\alpha_t = \alpha_{fc}\Gamma n + \alpha_s + (1 - \Gamma)\alpha_0 \quad (5)$$

where α_{fc} is the free-carrier absorption coefficient within the active region, α_s is the loss due to scattering, and α_0 is the free-carrier loss in the cladding regions. All constants and parameters are given in Table I.

B. Tapered Device Structure

The semiconductor laser contains three distinct regions—one with a constant active region width, a tapered region with a linearly decreasing active width, and a passive section with no active contact whatsoever. The curve and angle in the active region serve only to reduce the reflectivity, and so it can be straightened out for the purposes of the model, with the reflectivity value at the right hand facet R_3 set appropriately at 8×10^{-6} .

The model moves across the length of the device in a number of steps to create a number of sections. Each section in the active region has an associated width and surface area, which will be constant in the untapered region but variable in the tapered section. The two parameters that might be expected to depend upon the width or area of the active region within a particular section are the current density J and the optical confinement factor Γ . However, previously reported models of tapered devices have had conflicting methods of dealing with these values.

In other work, a constant current density has been assumed throughout a tapered active region, together with a constant optical confinement factor [10], [11]. Other methods have involved deriving the current density as a varying quantity depending

upon the electron density-dependent voltage across each section and its associated series resistance, while assuming either a fixed confinement factor [12], [13] or a variable one [14].

In terms of the optical confinement factor, the physically correct implementation is that of a variable factor within the photon density rate equation. This is because Γ represents a combination of the lateral and transverse confinement that is taking place. The transverse confinement is constant along the length of the active region, as it depends upon the vertical structure of the active region that does not alter. The lateral confinement is affected, however, as the width of the active region varies along the length. The confinement factor needs to be calculated at each point along the active region, and is, therefore, implemented appropriately in this model. Using proprietary software to calculate the total confinement factor, a maximum value of 0.079 in the widest part of the waveguide and 0.006 in the narrowest region has been derived.

Referring now to the current density J within the electron density rate (1), this model implements a varying value through the tapered active region. The photograph in Fig. 1 shows that, although the active material in the device is tapered, the electrical contact on top of the device is not. Therefore, it is a reasonable assumption that the electrical current is distributed evenly across this contact. Sections of the device within the tapered region, therefore, have the same amount of electrical current per section as the untapered region, but this is focused down into a smaller area of the active material and so results in a higher current density. Voltage and resistance values for each section of the device are not available, and so a simple calculation is made instead, based upon the assumption that an equal amount of electrical current passes through each section of the device, with the sum of these currents adding up to the total current.

The passive section of the device has no current passing through it at all, and so the electron density within it can be ignored. The photon density propagation is simply represented by a fixed loss term α_p , which includes the effects of optical confinement within the passive waveguide.

C. Grating Effects

Parameters for the gain approximation (4) were determined experimentally by using a Fabry–Perot laser of identical geometry and material to the untapered active region of the experimental device, with a length of approximately $500 \mu\text{m}$. The technique of Hakki and Paoli [15] was used together with the correction of Westbrook [16] to calculate material gain from the peak-to-trough ratios of longitudinal modes obtained below threshold. Data was taken at eight different currents, with Fig. 3 showing the resulting material gain curve obtained at four of these values.

In the mode-locking experiment, the grating selects a wavelength approximately 15 nm shorter than the peak emission. The material gain at this detuning was, therefore, extracted from the results and plotted against estimated carrier density for each of the eight currents. A best fit curve of the gain approximation was then obtained to yield the final gain curve parameters of $g_0 = 2935 \text{ cm}^{-1}$ and $n_{tr} = 1.21 \times 10^{18} \text{ cm}^{-3}$.

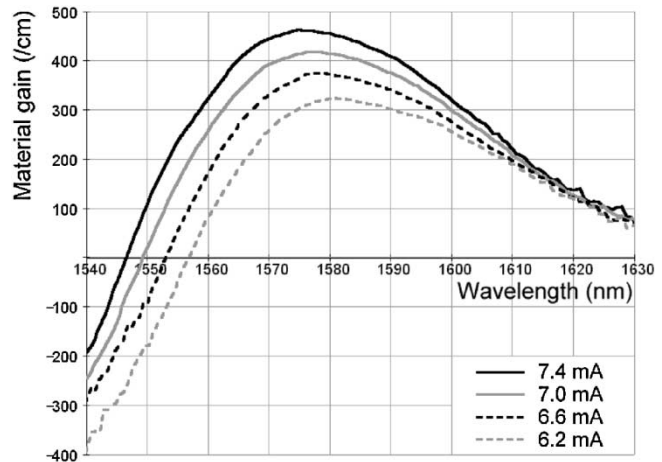


Fig. 3. Material gain curve obtained at four currents below threshold.

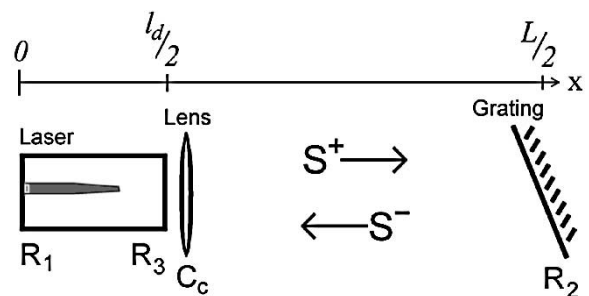


Fig. 4. Schematic of the modeled setup, indicating reflection and coupling coefficients and the direction of the photon density waves.

D. Saturable Absorber

Within the absorber section of the split contact device, the electron lifetime will be reduced as the drift current will dominate the diffusion current and electrons will be extracted from the device. The implementation of a $50\text{-}\mu\text{m}$ absorber section in this model is based upon the work of Avrutin [17], with the current density in the absorber region being set as zero, while the electron lifetime and gain values are adjusted to account for the negative current flow. In this model, the electron lifetime is reduced by increasing the trap recombination coefficient by a factor, denoted as C_{factor} . Within the absorber section, the gain is automatically moved to a region of loss on the material gain curve, due to the reduction in electron density caused by the zero current density and increase in trap recombination coefficient.

E. Method of Solution

The device is divided into 100 position steps $10 \mu\text{m}$ in length ($= \Delta x$), with the time step Δt set as the time taken for light to travel $10 \mu\text{m}$ in the semiconductor. The dc bias is applied first, with the time-independent (i.e., $dn/dt = 0$) rate equations being solved throughout the cavity until a steady-state solution is reached for photon density and electron density at each position in the semiconductor laser.

The RF is then switched on to initiate the mode-locking process, with the current density taking upon the previously defined time-dependent form $J(t)$. $t = 0$ solutions are taken as

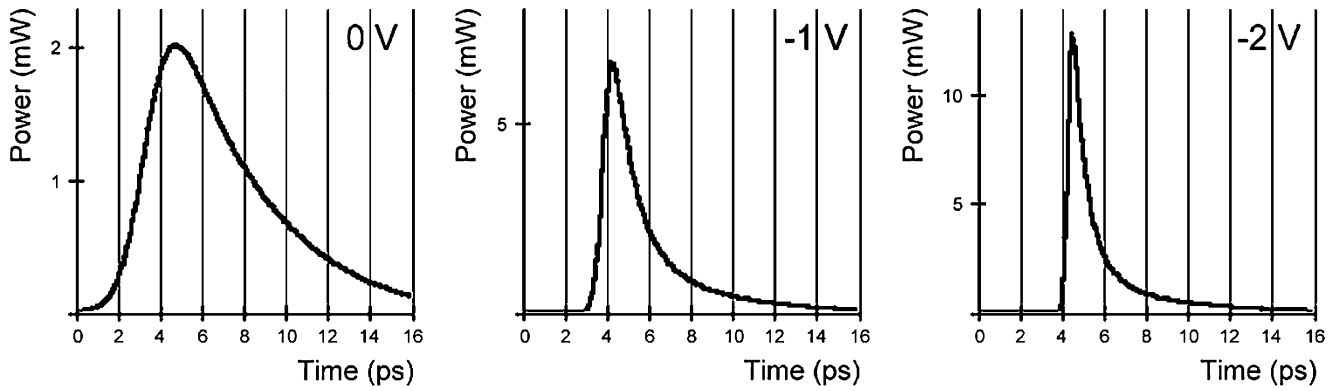


Fig. 5. Modeled pulse outputs with a grounded contact (0 V) and reverse-biased cases of -1 and -2 V. Pulsewidths are 5.5, 2.0, and 1.0 ps, respectively.

those derived for the static solution, with time then incremented by Δt and the rate equations solved throughout the cavity by the following relations:

$$\begin{aligned} n(x, t) &= n(x, t - \Delta t) + \Delta t \frac{\partial n(x, t - \Delta t)}{\partial t} \\ S^\pm(x, t) &= S^\pm(x \mp \Delta x, t - \Delta t) \\ &\quad + \Delta x \frac{\partial S^\pm(x \mp \Delta x, t - \Delta t)}{\partial x}. \end{aligned} \quad (6)$$

The boundary conditions are set with reference to the modeled setup of Fig. 4 as

$$\begin{aligned} S^+(0, t) &= R_1 S^-(0, t) \\ S^-\left(\frac{l_d}{2}, t\right) &= (1 - R_3)^2 C_c^2 R_2 S^+\left(\frac{l_d}{2}, t - t_{\text{ext}}\right) \\ &\quad + R_3 S^+\left(\frac{l_d}{2}, t\right) \end{aligned} \quad (7)$$

where t_{ext} is the external cavity round-trip time of the 2.5-GHz setup, and all other parameters are defined in Table I and Fig. 4.

When n and S have been calculated for all values of x , time is incremented by Δt and the process is repeated. To optimize the resulting optical pulses, it is necessary to finetune J_{dc} and J_{rf} , as well as the detuning, Δf , of ω from the exact round-trip frequency. After around 600 round-trips through the cavity the results are found to reach a steady solution with identical pulses being emitted for each cavity period and intensity fluctuations of less than 0.01%.

V. MODELING RESULTS

A. Open Circuit and Grounded Contact

In the open circuit active mode-locking case, the model gives 5.5-ps pulses at 2.5 GHz, with driving conditions of $J_{\text{dc}} = 0.38J_{\text{th}}$, $J_{\text{rf}} = 2.36J_{\text{th}}$, and $\Delta f = 0.6$ MHz, where J_{th} is the threshold current density of 1808 A/cm², equivalent to around 12 mA. At higher dc bias levels the pulse widths increase, and the 5.5-ps pulses represent the shortest possible pulses obtainable from the modeled setup. The dc bias level is lower than that of the experiment, but this set of driving conditions is only being used as a reference point for the ultimate pulse performance and so the relative values of the dc and RF currents will not be considered.

To replicate experimental conditions where the maximum RF power is used in all experiments, J_{rf} is now fixed at the value of $2.36 J_{\text{th}}$ so that any improvements in pulsewidth will be solely due the introduction of a saturable absorber.

A C_{factor} of 20 in the 50- μm absorber region has been found to give 5.5-ps hybrid mode-locking pulses, with a gradual increase in dc bias mimicking the experimental behavior with a sudden turn-on of pulses occurring at a certain value—in this modeled case at around $J_{\text{dc}} = 1.54J_{\text{th}}$. This indicates that the modeling approach is successfully simulating a saturation of the absorber region as observed in the experiment. Also, a negative frequency detuning of $\Delta f = -2.2$ MHz was required for optimum operation, which again supports the fact that hybrid mode-locking is taking place. That is because the absorption function delays the output of the pulse in the round-trip period, and, therefore, negative frequency detuning is required to cause the pulse to be emitted earlier in the round-trip period to coincide with the optimum emission position.

Lower values of C_{factor} cause an increase in pulsewidth, and higher values cause a decrease, with the specific value of 20 being chosen as it yields pulses that are similar to the active mode-locking situation. This is the approximate case with the experimental results, where grounding the contact only had a small effect on pulsewidths.

B. Reverse Biased Contact

As previously mentioned, reliable reverse biasing of the 50- μm contact was not achievable in the experiment. However, the model can now be used to simulate how pulsewidths could be improved if reverse biasing was possible.

The $C_{\text{factor}} = 20$ case is used as the reference point for a grounded contact. The electron lifetime in this absorber region was calculated to be approximately 450 ps, in comparison to 800 ps in the gain region. Karin *et al.* performed an experimental investigation into the dependence of the electron lifetime in a split contact absorber region with increasing reverse bias and found an exponential relationship [18]. Using this result together with the grounded lifetime of 450 ps as the value at a reverse bias of 0 V, the lifetimes at a variety of reverse bias voltages can be determined.

A -1 V reverse bias was found to correspond to a lifetime of 287 ps and a C_{factor} of 33, with a -2 V bias giving a lifetime reduction to 175 ps and a C_{factor} of 55. Both cases were

TABLE II
HYBRID MODE-LOCKING PULSES

C_{factor}	Bias (V)	J_{dc} ($\times J_{th}$)	Δf (MHz)	Pulse width (ps)	Rise time (ps)	Fall time (ps)
N/A	N/A	0.38	+0.6	5.5	5.3	5.7
20	0	1.54	-2.2	5.5	2.3	9.1
33	-1	1.74	-1.6	2.0	0.8	4.7
55	-2	2.08	-1.2	1.0	0.3	2.5

then modeled, with $J_{rf} = 2.36J_{th}$ fixed again, and the resulting pulse statistics are given in Table II with the pulse profiles shown in Fig. 5.

The dc pulse turn-on levels increase with increasing reverse bias, indicating that more absorption is present as would be expected. The shorter electron lifetime in the absorber with increasing reverse bias means that the absorber recovers quicker, hence narrowing the region of net gain experienced and shortening the pulses down to as little as 1.0 ps with a reverse bias of -2 V. Hybrid mode-locking effects are also revealed by strongly asymmetric pulses, with fall times that are 4–6 times greater than the rise times. This is due to the different pulse shaping effects being experienced, with the rising edge being shortened due to the initial loss in the absorber, while the falling edge is shortened to a lesser extent by the saturation of the gain and recovery of the absorber [19], [20].

The results compare very well with those reported in experimental work by Yvind *et al.* [21]. Their MQW device had a $550\text{-}\mu\text{m}$ gain section and a $50\text{-}\mu\text{m}$ absorber section, giving pulses of approximately 3.2-ps duration with a grounded contact. This reduced down to 2 ps at a -1 V bias on the absorber section, and 1.2 ps at -1.8 V, demonstrating similar improvements in pulsewidth to those discovered by this modeling work.

These results clearly demonstrate that if the experimental split contact device could be reliably reverse biased, the pulse widths obtainable should be considerably shorter than those obtained by the experimental work to date.

VI. SUMMARY

Hybrid mode-locking has been demonstrated for a semiconductor laser with a curved and tapered active region and a split contact. Grounding the $50\text{-}\mu\text{m}$ absorber contact gave pulses of approximately 5.5 ps in the experiment, which were comparable to those previously obtained with a single-contact device.

A traveling-wave rate-equation model has been developed, incorporating a variable current density and optical confinement factor along the cavity length to account for the tapered structure. Material gain parameters for the model were experimentally obtained, and the saturable absorber region was simulated by an increase in trap recombination throughout the $50\text{-}\mu\text{m}$ contact region. Use of the model indicated that hybrid mode-locking pulse widths could be reduced from 5.5 ps down to 2.0 ps and 1.0 ps with reverse bias voltages of -1 and -2 V, respectively.

ACKNOWLEDGMENT

The authors are grateful to Corning for supplying devices and to A. Ellis, A. Borghesani, and S. Dudley for helpful discussions.

REFERENCES

- [1] M. Schell, A. G. Weber, E. Schöll, and D. Bimberg, "Fundamental limits of sub-ps pulse generation by active mode-locking of semiconductor-lasers—The spectral gain width and the facet reflectivities," *IEEE J. Quantum Electron.*, vol. 27, pp. 1661–1668, June 1991.
- [2] C. A. Williamson, M. J. Adams, A. D. Ellis, and A. Borghesani, "Mode-locking of semiconductor laser with curved waveguide and passive mode expander," *Appl. Phys. Lett.*, vol. 82, no. 3, pp. 322–324, Jan. 2003.
- [3] I. F. Lealman, A. E. Kelly, L. J. Rivers, S. D. Perrin, and R. Moore, "Improved gain block for long wavelength ($1.55\text{ }\mu\text{m}$) hybrid integrated devices," *Electron. Lett.*, vol. 34, no. 23, pp. 2247–2249, Nov. 1998.
- [4] P. Doussiere, P. Garabedian, C. Graver, E. Derouin, E. Gaumont-Goarin, G. Michaud, and R. Meilleur, "Tapered active stripe for $1.5\text{-}\mu\text{m}$ InGaAsP/InP strained multiple quantum well lasers with reduced beam divergence," *Appl. Phys. Lett.*, vol. 64, no. 5, pp. 539–541, Jan. 1994.
- [5] J. Chung and A. M. Weiner, "Ambiguity of ultrashort pulse shapes retrieved from the intensity autocorrelation and the power spectrum," *IEEE J. Select. Topics Quantum Electron.*, vol. 7, pp. 656–666, July/Aug. 2001.
- [6] M. S. Demokan, "A model of a diode laser actively mode-locked by gain modulation," *Int. J. Electron.*, vol. 60, no. 1, pp. 67–85, Jan. 1986.
- [7] J. E. Bowers, P. A. Morton, A. Mar, and S. W. Corzine, "Actively mode-locked semiconductor lasers," *IEEE J. Quantum Electron.*, vol. 25, pp. 1426–1439, June 1989.
- [8] P. W. A. McIlroy, A. Kurobe, and Y. Uematsu, "Analysis and application of theoretical gain curves to the design of multi-quantum-well lasers," *IEEE J. Quantum Electron.*, vol. 21, pp. 1958–1963, Dec. 1985.
- [9] L. A. Coldren and S. W. Corzine, *Diode Lasers and Photonic Integrated Circuits*. New York: Wiley, 1995.
- [10] P. W. Tan and H. Gafouri-Shiraz, "Sub-picosecond gain dynamic in highly index-guided tapered-waveguide laser diode optical amplifiers," *Proc. Inst. Elect. Eng.*, pt. J, vol. 146, no. 2, pp. 83–88, Apr. 1999.
- [11] W. M. Wong and H. Gafouri-Shiraz, "Dynamic model of tapered semiconductor lasers and amplifiers based on transmission-line laser modeling," *IEEE J. Select. Topics Quantum Electron.*, vol. 6, pp. 585–593, July/Aug. 2000.
- [12] R. J. Lang, A. Hardy, R. Parke, D. Mehuys, S. O'Brien, J. Major, and D. Welch, "Numerical analysis of flared semiconductor laser amplifiers," *IEEE J. Quantum Electron.*, vol. 29, pp. 2044–2051, June 1993.
- [13] K. A. Williams, R. V. Pentyl, I. H. White, D. J. Robbins, F. J. Wilson, J. J. Lewandowski, and B. K. Nayar, "Design of high-brightness tapered laser arrays," *IEEE J. Select. Topics Quantum Electron.*, vol. 5, pp. 822–831, May/June 1999.
- [14] G. P. Agrawal, "Fast-Fourier-transform based beam-propagation model for stripe-geometry semiconductor lasers: inclusion of axial effects," *J. Appl. Phys.*, vol. 56, no. 11, pp. 3100–3109, Dec. 1984.
- [15] B. W. Hakki and T. L. Paoli, "Gain spectra in GaAs double-heterostructure injection lasers," *J. Appl. Phys.*, vol. 46, no. 3, pp. 1299–1306, Mar. 1975.
- [16] L. D. Westbrook, "Measurements of dg/dN and dn/dN and their dependence on photon energy in $\lambda = 1.5\text{ }\mu\text{m}$ InGaAsP laser diodes," *Proc. Inst. Elect. Eng.*, pt. J, vol. 133, no. 2, pp. 135–142, Apr. 1986.
- [17] E. A. Avrutin, "Analysis of spontaneous emission and noise in self-pulsing laser diodes," *Proc. Inst. Elect. Eng.*, pt. J, vol. 140, no. 1, pp. 16–20, Feb. 1993.
- [18] J. R. Karin, R. J. Helkey, D. J. Derickson, R. Nagarajan, D. S. Allin, J. E. Bowers, and R. L. Thornton, "Ultrafast dynamics in field-enhanced saturable absorbers," *Appl. Phys. Lett.*, vol. 64, no. 6, pp. 676–678, Feb. 1994.
- [19] H. A. Haus, "Theory of forced mode locking with a slow saturable absorber," *IEEE J. Quantum Electron.*, vol. QE-11, pp. 736–746, 1975.
- [20] R. A. Salvatore, T. Schrans, and A. Yariv, "Pulse characteristics of passively mode-locked diode lasers," *Opt. Lett.*, vol. 20, no. 7, pp. 737–739, Apr. 1995.
- [21] K. Yvind, P. M. W. Skovgaard, J. Mørk, J. Hanberg, and M. Kroh, "Performance of external cavity mode-locked semiconductor lasers employing reverse biased saturable absorbers," *Physica Scripta*, vol. T101, pp. 129–132, 2002.

Craig A. Williamson was born in Keighley, U.K., in 1976. He received the M.Phys. degree from the University of Lancaster, Lancaster, U.K., in 1998 and the Ph.D. degree in applied physics from the University of Essex, Colchester, U.K., in 2003. He is currently working toward the Ph.D. degree at the University of Essex, Colchester, U.K.

He has experience in optical networking technologies from his time as a Research Scientist at BT Laboratories, Ipswich, U.K., and as a Technical Writer with *Light Reading* magazine. His main interest at present is the mode locking of semiconductor lasers for telecommunications applications.

Mr. Williamson is a member of the Institute of Physics, U.K., and has achieved Chartered Physicist status.

Michael J. Adams received the Ph.D. degree in laser theory in 1970.

He has worked in optoelectronics R&D with 15 years experience in industry (Plessey, BT), and 17 years in academia (Universities of Cardiff, Southampton, and Essex, U.K.). Since 1996, he has been a Professor at the University of Essex, Colchester, U.K. His research interests include semiconductor lasers, optical amplifiers, optical waveguides, optical bistability, semiconductor nonlinear optics and optical switching devices, and nonlinear dynamics of lasers. He has published widely in the optoelectronics field over many years, including a standard text on optical waveguide theory and two books on semiconductor lasers and optical fibers for use in telecommunications. He serves as Honorary Editor of *Proceedings of the Institution of Electrical Engineers, Optoelectronics*, and is a Member of Editorial Advisory Board of the *International Journal of Numerical Modeling*.